14th International Conference on Applications of Statistics and Probability in Civil Engineering, ICASP14
Dublin, Ireland, July 9-13, 2023

Framework for probabilistic connectivity estimation of bridge networks under seismic and flood hazards

Putri S. Firdaus and Koki Aoki
Doctoral Student, Dept. of Civil and Environmental Engineering, Waseda University, Tokyo, Japan

Hiroshi Matsuzaki
Associate Professor, Dept. of Civil and Environmental Engineering, National Defense Academy of Japan, Kanagawa, Japan

Mitsuyoshi Akiyama
Professor, Dept. of Civil and Environmental Engineering, Waseda University, Tokyo, Japan

Dan M. Frangopol
Professor, Dept. of Civil and Environmental Engineering, ATLSS Engineering Research Center, Lehigh University, Bethlehem, PA, USA

ABSTRACT: Bridges play a crucial role in post-disaster rescue and recovery operations as an essential component in road networks. As observed in recent earthquakes and floods, the road closure due to damage of bridges has emphasized the importance of investigating the entire civil infrastructure system and networks. This paper presents a framework for estimating the probabilistic connectivity of bridge networks under seismic and flood hazards. The proposed method can provide a relevant strategy to maximize the connectivity of the road network, considering the differences in hazard intensity and bridge vulnerability. It is confirmed in an illustrative example that large lateral strength of bridge columns can contribute to ensuring the connectivity of the road network under both seismic and flood hazards.

1. INTRODUCTION

Bridges are an essential component of highway transportation networks. They have been regarded as one of the most vulnerable road structures in the network when subjected to natural disasters. Damage to bridges degrades network functionality, disrupting the transportation of emergency goods as well as post-disaster rescue and recovery efforts. Among natural hazards, an earthquake has been widely perceived as a major threat due to its destructive impacts on civil infrastructures. During the 2011 Great East Japan earthquake, for example, there were approximately 2300 km of the highway closed due to ground motion-induced bridge damage (Nojima & Kato, 2013).

Furthermore, climate change has become a growing concern for bridges exposed to hydrometeorological events (e.g., floods and hurricanes) (Yang & Frangopol, 2019). Extreme floods have been reported to induce damage to riverine bridges (Liao et al., 2016), which consequently render transportation network deterioration, as observed in the 2020 Kyushu flood (Liu et al., 2021; Mukunoki et al., 2021). Several studies have addressed issues associated with bridge networks under natural hazards (Ishibashi et al., 2020; Liu et al., 2020; Liu & Frangopol, 2005; Han & Frangopol 2022). To investigate the functionality of a road network under seismic and flood hazards, the damage level of individual bridges was a key metric in the literature. However, the spatial correlation associated with hazard intensity (i.e., peak ground velocity and flow discharge) over the road network has not been addressed in the connectivity assessment.

This paper presents a framework to estimate the probabilistic connectivity of bridge networks under seismic and flood hazards considering the

spatial correlations. The proposed framework is not only able to suggest an optimal disaster mitigation strategy but also evaluate the effect of bridge vulnerability on the network connectivity. As an illustrative example, the proposed framework is applied to a hypothetical bridge network in Hitoyoshi City, Japan, where disastrous earthquakes and floods have been repeatedly observed.

2. FRAMEWORK FOR PROBABILISTIC CONNECTIVITY ESTIMATION OF BRIDGE NETWORKS UNDER SEISMIC AND FLOOD HAZARDS

Figure 1 presents the proposed framework for estimating the probabilistic connectivity of bridge networks under seismic and flood hazards. In this study, seismic and flood hazards are assumed to be statistically independent. Details are provided below.

2.1. Network topology

The configuration of an intact bridge network G is portrayed as an arbitrary graph in Equation (1), as defined by Aoki et al. (2022).

$$G(V,E) \quad E \subseteq \{uv | v \in V, u \neq v\} \tag{1}$$

where V is a subset of vertices that represent origin-destination (OD) pairs and individual bridges, and E is a subset of links or routes connecting nodes uv.

2.2. Seismic hazard assessment

Peak ground velocity (PGV) is chosen as the intensity measure to quantify seismic hazard. The PGV at the ground surface is calculated by using the peak bedrock velocity (PBV), which can be evaluated using Equation (2) proposed by Si & Midorikawa (1999) and an amplification factor (AF). The engineering bedrock is defined as a shear-wave velocity of 600 m/s.

$$\log(PBV) = 0.58M_w + 0.0038H - 1.29 \quad -\log\left(X + 0.0028 \times 10^{0.59M_w}\right) \quad -0.002X + \varepsilon \tag{2}$$

where M_w is the moment magnitude, H is the depth of the fault at the center, X is the fault distance, and ε is the variable associated with the attenuation rule that follows a normal random number with mean zero and standard deviation of 0.23.

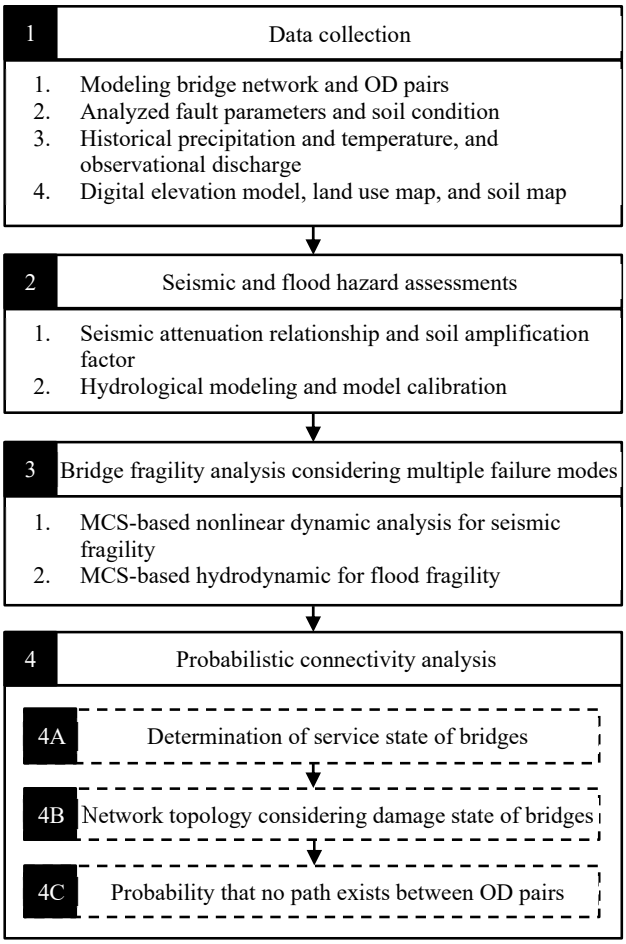

Figure 1. Framework for probabilistic connectivity estimation of bridge networks under seismic and flood hazards

AF proposed by Fujimoto & Midorikawa (2006) is used in this study.

$$\log(AF) = -0.852\log\left(\frac{AVS_{30}}{V_{S,B}}\right) \tag{3}$$

where AVS_{30} is the average shear-wave velocity at a depth of 30 m below the surface, and $V_{S,B}$ = 600 m/s is the shear-wave velocity at the engineering bedrock.

ε in Equation (2), which determines the peak bedrock velocity at bridge locations in the road network, is evaluated considering the spatially fully correlated or fully independent case.

2.3. Flood hazard assessment

Annual peak flow (Q_A) has been selected as the intensity measure in the literature when estimating the reliability of bridges exposed to flooding (Dong & Frangopol, 2017; Yang & Frangopol, 2019). To obtain Q_A, the daily time series of flow discharge is simulated using hydrologic modeling. In the proposed approach, the Soil Water Assessment Tool (SWAT), a semi-distributed physics-based hydrological model that can predict the hydrologic response of an ungauged watershed developed by Arnold et al. (2012), is adopted.

2.4. Fragility of bridges under seismic and flood hazards

The seismic fragility curve is developed using the limit states associated with the flexural and shear failures of the bridge column. Their performance functions are as follows:

$$g_{s1} = \alpha_{dc}\delta_c - \delta_{max} \tag{4}$$

$$g_{s2} = \alpha_{sc}V_c + \alpha_{ss}V_s - V_{d,e} \tag{5}$$

where δ_c is the ultimate displacement capacity of RC columns (Public Works Research Institute, 2013), α_{dc} is the model uncertainty associated with the estimation of δ_c, δ_{max} is the response displacement of RC columns, V_c and V_s are the shear resistances of the concrete and reinforcement contributions, respectively, $V_{d,e}$ is the shear force acting on the column during earthquake excitation, and α_{sc} and α_{ss} are the model uncertainties associated with the bearing capacity estimations.

Although flexural failure could occur in bridge columns due to the water flow during floods, it is difficult to calculate the plastic deformation of the RC columns. Therefore, for flood fragility, a comparison of the flexural capacity and the bending moment demand is performed. The performance functions of the bridge column are provided by Equations (6) and (7).

$$g_{f1} = M_y - M_d \tag{6}$$

$$g_{f2} = \alpha_{sc}V_c + \alpha_{ss}V_s - V_{d,f} \tag{7}$$

where M_y is the yield bending moment of the column, M_d and $V_{d,f}$ are the demands of the moment at the column base and the shear force acting on the column, respectively, produced by flow-induced pressure.

During an extreme flood event, the bridge superstructure is completely submerged, and the horizontal and vertical forces acting on the bearings exceed their capacity, causing the washout of the superstructure. The associated performance functions are provided by:

$$g_{f3} = \alpha_{ub}F_{sb} - F_{dd} \tag{8}$$

$$g_{f4} = \alpha_{ub}F_{vb} - (F_{ld} + F_{bd}) \tag{9}$$

where α_{ub} represents the model error associated with the ultimate bearing strength, F_{sb} and F_{vb} are the shear and tensile bearing strengths, respectively, F_{bd} is the buoyancy force, and F_{dd} and F_{ld} are the drag and lift forces acting on the bridge deck, respectively, calculated using the method proposed by Kerenyi et al. (2009).

Monte-Carlo simulation (MCS) is employed to estimate the fragility of bridges considering the associated uncertainty.

2.5. Probabilistic network connectivity

In catastrophic events, bridges in a transportation network may become inoperative. Bocchini & Frangopol (2011) specified the in/out state of individual bridges after such events (s_b) as a binary variable provided by Equation (10).

$$s_b = \begin{cases} 1, & \text{if } P_{bn}(\gamma_{bn}|g \le 0) \ge q_{vbn}(\text{impassable}) \\ 0, & \text{if } P_{bn}(\gamma_{bn}|g \le 0) < q_{vbn}(\text{passable}) \end{cases} \tag{10}$$

where P_{bn} is the conditional failure probability given hazard intensity γ_{bn}, g is the performance function given by Equations (4) and (5) for bridges under seismic hazard and Equations (6) to (9) for bridges under flood hazard, and q_{vbn} is a random number between 0 and 1, which is associated with hazard-induced damage.

The network connectivity in this study was developed following the framework provided by

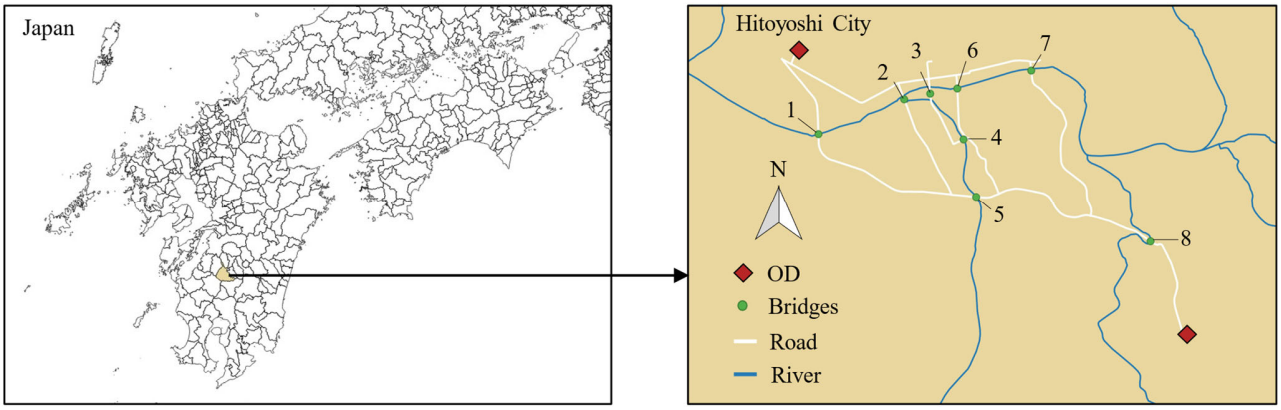

Figure 2. Study area and topology of the analyzed hypothetical bridge network

Aoki et al. (2022). Their framework adopted Dijkstra's algorithm (Dijkstra, 1959) in the calculation of disconnected network probability.

3. ILLUSTRATIVE EXAMPLE

3.1. Study area

Figure 2 depicts a hypothetical bridge network in Hitoyoshi City, Kumamoto Prefecture, Japan. It is comprised of 8 riverine bridges that connect an OD pair and are subjected to seismic and flood hazards.

Hitoyoshi city is divided into northern and southern parts by the Kuma River, which is known as one of the three swiftest rivers in Japan. Moreover, the southern boundary fault of the Hitoyoshi basin, which would cause a large earthquake with a moment magnitude of more than 6.5, is located near Hitoyoshi City. Table 1 lists the local attributes of the considered bridges. The main channel section or reach number is generated using watershed delineation in SWAT.

3.2. Model bridges

Table 2 presents the structural details of bridge columns located on the medium soil used in this study, which are designed according to Japanese design codes published in 1964 and 2017 (hereafter, 1964 bridge and 2017 bridge, respectively). The 1964 bridges have inadequate amount of shear reinforcement, which causes brittle failure when subjected to strong seismic motion. The 2017 bridges designed considering large seismic action (e.g., the 1995 Kobe earthquake) have high seismic performance with adequate ductility capacity. In addition, the bearing properties are adopted from Ishibashi et al. (2020).

Table 3 summarizes the uncertainties associated with the material strengths, calculation of column capacities, and stream flow estimation, assuming normal distribution for all random variables considered. The effect of seismic performance on the reliability of bridges in the flood-prone region is investigated herein.

Table 1. Local attributes

Site number	*Reach number*	*Reach slope (%)*	*AVS_{30} (m/s)*
1	*15*	*0.45*	*321.9*
2	*16*	*0.03*	*311.4*
3	*16*	*0.03*	*323.1*
4	*23*	*1.69*	*353.4*
5	*23*	*1.69*	*355.1*
6	*16*	*0.03*	*322.6*
7	*16*	*0.03*	*334.8*
8	*22*	*1.24*	*405.6*

Table 2. Structural details of model bridge columns

	1964 bridge	*2017 bridge*
Cross-section (mm)	*3600×2400*	*3800×2400*
ρ_l (%)	*0.67*	*1.3*
ρ_s (%)	*0.14*	*1.0*

Note: ρ_l = longitudinal reinforcement ratio, and ρ_s = volumetric tie ratio

Table 3. Parameters of random variables in the fragility assessment

	Mean	*COV*
Mass	*1.05*	*0.05*
Concrete compressive strength	*1.20*	*0.10*
Yield strength of reinforcement	*1.20*	*0.07*
Young's modulus of reinforcement	*0.97*	*0.01*
α_{dc}	*1.062*	*0.181*
α_{sc}	*1.02*	*0.082*
α_{ss}	*1.22*	*0.145*
k_v	*1.00*	*0.15*

Note: COV = coefficient of variation

3.3. Seismic hazard assessment

Figure 3 shows the seismic hazard curves. Hazard curves evaluated as probabilities of exceedance over 30 years obtained from the Japan Seismic Hazard Information Station (J-SHIS) of National Research Institute for Earth Science and Disaster Resilience (NIED) were converted into the annual probability of exceedance assuming Poisson's model. In addition, the information on AVS_{30} to calculate AF in Equation (3) was obtained from Wakamatsu & Matsuoka (2013). Figure 3 shows a slightly higher seismic hazard at Sites 5 and 8, which have relatively smaller fault distances compared to Sites 1 and 4.

3.4. Flood hazard assessment

The Kuma River watershed was modeled in SWAT hydrologic modeling to simulate daily discharges. The spatial distributions of the slope, land use, and soil information were retrieved from the United States Geological Survey (USGS) Earth Explorer (USGS, 2000), the directory of the Ministry of Land, Infrastructure, Transport, and Tourism in Japan (MLIT, 2016), and the Harmonized World Soil Database (FAO/IIASA/ISRIC/ISSCAS/JRC, 2012), respectively. The daily time series of precipitation and temperature were obtained from Japan Meteorological Agency (JMA) weather record.

Due to the lack of observational data, only Reach 16 was calibrated according to the recorded daily discharge from the water information system of MLIT. Figure 4 displays the flood hazard curves of the reaches listed in Table 1.

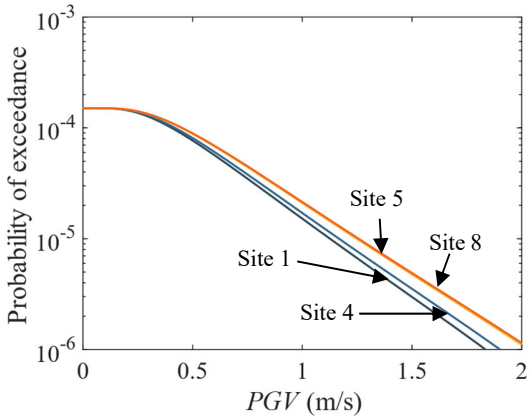

Figure 3. Seismic hazard curves

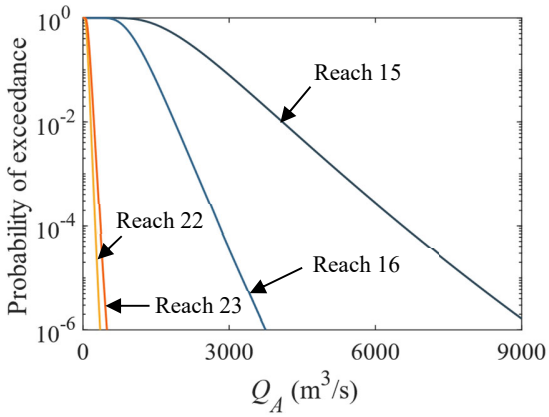

Figure 4. Flood hazard curves

3.5. Seismic fragility assessment

Seismic fragility assessment was conducted using a total of 18 horizontal components of ground motions recorded during inland earthquakes caused by active faults with a PGV of 0.50 m/s or more at the sites located on medium soil in Japan. The time-history non-linear dynamic analysis of the RC bridge columns was conducted using a one-degree-of-freedom (1DOF) with Takeda's degrading stiffness model (Takeda et al., 1970).

Figure 5 shows the seismic fragility curves. The 1964 bridge is prone to shear failure even at small seismic intensities, whereas the 2017 bridge has a smaller probability of failure due to sufficient ductility capacity.

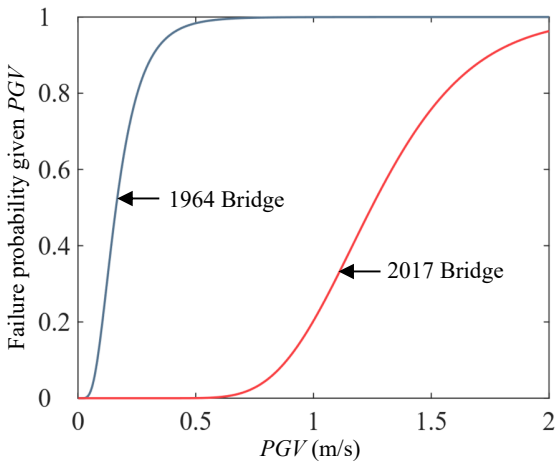

Figure 5. Seismic fragility curves

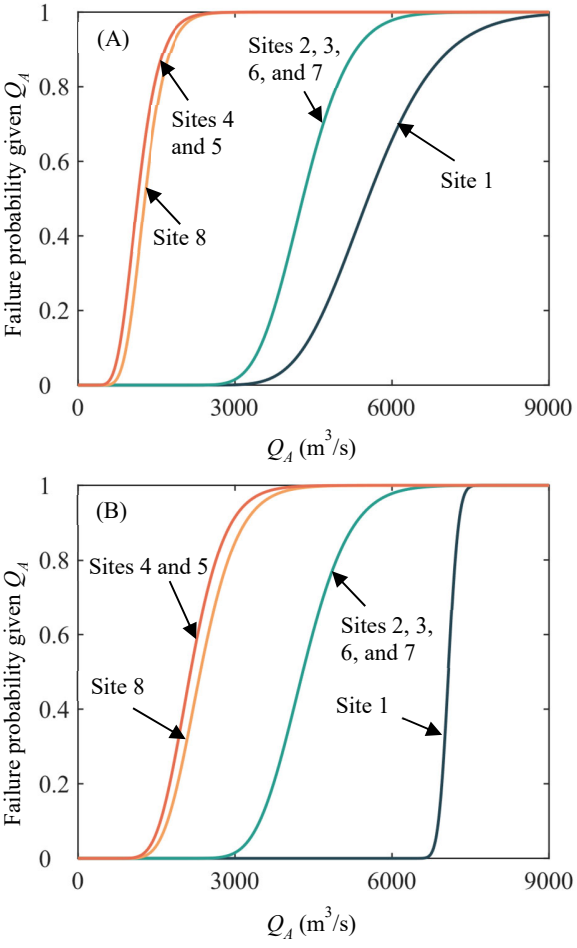

Figure 6. Flood fragility curves: (A) 1964 Bridge and (B) 2017 Bridge

3.6. Flood fragility assessment

The bridges listed in Table 1 are located at the mainstream (i.e., Reach 15 and 16) and the tributaries (i.e., Reach 22 and 23) of the Kuma River. The mainstream is assumed to have a compound channel cross-section with a channel span equal to 80 m, while the tributaries are assumed to have a trapezoidal cross-section with a channel span equal to 40 m. It should be noted that these bridges are hypothetical and do not exist in Hitoyoshi City. The uncertainties associated with stream flow estimation and stream profile are considered using k_v in Table 3.

Figure 6 plots the flood fragility curves. A wider channel span suggests a larger area of cross-section, which generates less extreme flow velocities. Consequently, for bridges located on the mainstream, bridge fragility depends on the failure mode associated with the superstructure washout, whereas for bridges situated on the tributaries, it depends on the damage to the RC column. In addition, a steep channel slope exacerbates the flow velocity. This caused shear failure of the 1964 bridge at Site 1 because of insufficient amount of ties. It was confirmed that advanced seismic design methods contribute to improved reliability of bridges subjected not only to earthquake but also to flooding.

3.7. Road network probabilistic connectivity

To estimate the probabilistic connectivity of the bridge network, the spatial correlation both in hazard intensity and hazard-induced damage (i.e., q_{vbn} in Equation (10)) are considered. In this study, independent and perfect correlation assumptions are adopted.

Table 4 summarizes the disconnected probability of the analyzed road network, assuming that the network has only the 1964 or 2017 bridge models. The road network consisting of the 2017 bridges under seismic and flood hazards exhibits a substantially improved functionality compared to that consisting of the 1964 bridges for both perfect correlation and independent cases. The probability of disconnection between OD pairs for the independent case is higher than that for the perfect

correlation case. This is because in the perfect correlation case, all bridges in the route are damaged or they remain in sound condition, resulting in a smaller probability of disconnection between OD pairs.

The results of the probabilistic connectivity assessment of the analyzed road network suggest that disaster prevention measures should consider flood hazard as the dominant threat.

Table 4. Disconnected probability of the road network in Hitoyoshi City

Correlation case	*1964 bridges*	*2017 bridges*
Perfectly correlated (ground motion)	1.4×10^{-4}	1.6×10^{-5}
Perfectly correlated (flood)	2.6×10^{-3}	4.5×10^{-4}
Independent (ground motion)	1.5×10^{-4}	1.6×10^{-5}
Independent (flood)	2.7×10^{-3}	4.7×10^{-4}

4. CONCLUSIONS

A framework for estimating the probabilistic connectivity of bridge networks under seismic and flood hazards is presented. Differences in hazard intensity over the road network are considered in the proposed framework. The network connectivity depends on individual bridge failure due to earthquake excitation and/or flooding.

For the purpose of illustrative example, the proposed framework was applied to a hypothetical bridge network in Hitoyoshi City that is prone to seismic activity and extreme flooding. Increased lateral strength of bridge columns lowers the disconnected probability of the road network under both seismic and flood hazards. In addition, when the correlation of hazard-induced damage is spatially independent, the probability of disconnection between OD pairs is higher. The results of the probabilistic connectivity assessment demonstrated that the analyzed road network is more susceptible to flood hazard.

REFERENCES

Akiyama, M., Frangopol, D. M., & Ishibashi, H. (2020). Toward life-cycle reliability-, risk- and resilience-based design and assessment of bridges and bridge networks under independent and interacting hazards: emphasis on earthquake, tsunami and corrosion. *Structure and Infrastructure Engineering*, *16*(1), 26–50. https://doi.org/10.1080/15732479.2019.1604770

Aoki, K., Fuse, Y., Akiyama, M., Ishibashi, H., Koshimura, S., & Frangopol, D. M. (2022). Probabilistic connectivity assessment of bridge networks under seismic hazard considering the spatial correlation of ground motion-induced damage. In *Bridge Safety, Maintenance, Management, Life-Cycle, Resilience and Sustainability* (pp. 137–142). CRC Press. https://doi.org/10.1201/9781003322641-12

Arnold, J. G., Moriasi, D. N., Gassman, P. W., Abbaspour, K. C., White, M. J., Srinivasan, R., Santhi, C., Harmel, R. D., van Griensven, A., Liew, M. W. van, Kannan, N., Jha, M. K., Harmel, D., Member, A., Liew, M. W. van, & Arnold, J.-F. G. (2012). *SWAT: Model, calibration, and validation*. *55*(4), 1491–1508. http://swatmodel.tamu.edu

Bocchini, P., & Frangopol, D. M. (2011). Generalized bridge network performance analysis with correlation and time-variant reliability. *Structural Safety*, *33*(2), 155–164. https://doi.org/10.1016/j.strusafe.2011.02.002

Dijkstra, E. W. (1959). A note on two problems in connexion with graphs. *Numerische Mathematik*, *1*(1). https://doi.org/10.1007/BF01386390

Dong, Y., & Frangopol, D. M. (2017). Probabilistic assessment of an interdependent healthcare–bridge network system under seismic hazard. *Structure and Infrastructure Engineering*, *13*(1), 160–170. https://doi.org/10.1080/15732479.2016.1198399

FAO/IIASA/ISRIC/ISSCAS/JRC. (2012). *Harmonized World Soil Database (version 1.2)*.

Han, X., & Frangopol, D.M. (2022). Life-cycle connectivity-based maintenance strategy for bridge networks subjected to corrosion considering correlation of bridge resistances. *Structure and Infrastructure Engineering*, 18(12), 1614-1637. https://doi.org/10.1080/15732479.2021.2023590

Ishibashi, H., Akiyama, M., Frangopol, D. M., Koshimura, S., Kojima, T., & Nanami, K. (2020). Framework for estimating the risk and resilience of road networks with bridges and embankments under both seismic and tsunami hazards. *Structure and Infrastructure Engineering*, *17*(4), 494–514. https://doi.org/10.1080/15732479.2020.1843503

Japan Meteorological Agency. (n.d.). *Past weather data*. Retrieved January 21, 2021, from https://www.data.jma.go.jp/obd/stats/etrn/index.php

Kato, A., Nakamura, K., & Hiyama, Y. (2016). The 2016 Kumamoto earthquake sequence. *Proceedings of the Japan Academy Series B: Physical and Biological Sciences*, *92*(8), 358–371. https://doi.org/10.2183/pjab.92.359

Kerenyi, K., Sofu, T., & Guo, J. (2009). *Hydrodynamic Forces on Inundated Bridge Decks*. www.tfhrc.gov

Liao, K. W., Muto, Y., Chen, W. L., & Wu, B. H. (2016). A probabilistic bridge safety evaluation against floods. *SpringerPlus*, *5*(1). https://doi.org/10.1186/s40064-016-2366-3

Liu, L., Yang, D. Y., & Frangopol, D. M. (2020). Network-level risk-based framework for optimal bridge adaptation management considering scour and climate change. *Journal of Infrastructure Systems*, *26*(1), 04019037. https://doi.org/10.1061/(ASCE)IS.1943-555X.0000516

Liu, M., & Frangopol, D. M. (2005). Balancing connectivity of deteriorating bridge networks and long-term maintenance cost through optimization. *Journal of Bridge Engineering*, *10*(4), 468–481.

Liu, W., Maruyama, Y., & Yamazaki, F. (2021). Damage assessment of bridges due to the 2020 July flood in Japan using ALOS-2 intensity images. *2021 IEEE International Geoscience and Remote Sensing Symposium IGARSS*, 3809–3812. https://doi.org/10.1109/IGARSS47720.2021.9554001

MLIT. (n.d.). *Water Information System*. Retrieved June 21, 2021, from http://www1.river.go.jp/

MLIT. (2016). *Land Use Subdivision Mesh Data*. https://nlftp.mlit.go.jp/ksj/gml/datalist/KsjTmplt-L03-b.html

Mukunoki, T., Suetsugu, D., Sako, K., Murakami, S., Fukubayashi, Y., Ishikura, R., Hino, T., Sugimoto, S., Wakinaka, K., Ito, S., & Koyama, A. (2021). Reconnaissance report on geotechnical damage caused by a localized torrential downpour with emergency warning level in Kyushu, Japan. *Soils and Foundations*, *61*(2), 600–620. https://doi.org/https://doi.org/10.1016/j.sandf.2021.01.008

National Research Institute for Earth Science and Disaster Resilience. (n.d.). *Japan Seismic Hazard Information Station*. Retrieved September 27, 2021, from https://www.j-shis.bosai.go.jp/map/

Nojima, N., & Kato, H. (2013). Spatio-temporal analysis of traffic volumes on highway networks –comparison of the Great East Japan earthquake disaster and the Great Hanshin-Awaji earthquake disaster. *Journal of Japan Society of Civil Engineers, Ser. A1 (Structural Engineering & Earthquake Engineering)*, *69*(4), 121–133. https://doi.org/10.2208/jscejseee.69.I_121

Public Works Research Institute. (2013). Evaluation method for seismic limit states of reinforced concrete bridge columns, Technical Note of PWRI 4262.

Si, H., & Midorikawa, S. (1999). New attenuation relationships for peak ground acceleration and velocity considering effects of fault type and site condition. *Journal of Structural and Construction Engineering (Transactions of AIJ)*, *64*(523), 63–70. https://doi.org/10.3130/aijs.64.63_2

Takeda, T., Sozen, M. A., & Nielsen, N. N. (1970). Reinforced concrete response to simulated earthquakes. *Journal of the Structural Division*, *96*(12), 2557–2573. https://doi.org/10.1061/JSDEAG.0002765

USGS. (2000). *Earth Explorer*. https://earthexplorer.usgs.gov/

Wakamatsu, K., & Matsuoka, M. (2013). Nationwide 7.5-arc-second Japan engineering geomorphologic classification map and Vs30 zoning. *Journal of Disaster Research*, *8*(5). https://doi.org/10.20965/jdr.2013.p0904

Yang, D. Y., & Frangopol, D. M. (2019). Physics-based assessment of climate change impact on long-term regional bridge scour risk using hydrologic modeling: Application to Lehigh River watershed. *Journal of Bridge Engineering*, *24*(11), 04019099. https://doi.org/10.1061/(ASCE)BE.1943-5592.0001462